DOI:
10.1097/CCM.0000000000004141

Document Version
Peer reviewed version

Mechanical ventilation redistributes blood to poorly ventilated areas in experimental lung injury

John N. Cronin MBBS MSc MRCP FRCA [1], Douglas C. Crockett BVSc BMBCh FRCA MRCVS MRCP [2], Andrew D. Farmery MA MD FRCA [2], Göran Hedenstierna MD PhD [3], Anders Larsson MD PhD DEAA [4], Luigi Camporota MD PhD FRCP FFICM [1,5], Federico Formenti PhD DPhil [1,2]*

1. Centre for Human and Applied Physiological Sciences, King's College London, London, UK
2. Nuffield Division of Anaesthetics, University of Oxford, Oxford, UK
3. Hedenstierna Laboratory, Department of Medical Sciences, Uppsala University, Uppsala, Sweden
4. Hedenstierna Laboratory, Department of Surgical Sciences, Uppsala University, Uppsala, Sweden
5. Department of Adult Critical Care, St Thomas' Hospital, Guy's and St Thomas' NHS Foundation Trust, King's Health Partners, London, UK

* - corresponding author: Federico Formenti – email: federico.formenti@outlook.com, postal address: Centre for Human and Applied Physiological Sciences, Faculty of Life Sciences and Medicine, Shepherd's House, Guy's Campus, Kings College London, London, SE1 1UL, United Kingdom. Tel: +4420 7848 6292. Fax: +4420 7848 6325. Requests for reprints are accepted.

This work was undertaken at the Hedenstierna Laboratory, Uppsala University, Uppsala, Sweden.

Authors contributions: FF and AF generated the hypothesis, JNC, LC and FF designed the experiments, JNC, DC, FF, AL and GH performed the experiments, JNC analyzed the data, JNC, AL, LC and FF interpreted the data, AF, AL, GH and FF contributed to financial support. All authors critically revised the manuscript.

Conflicts of Interest and Sources of Funding: AF was supported by the Wellcome Trust (HMRXGK00), AL and GH were supported by the Swedish Lung and Heart Foundation (20170531) and the Swedish Research Council (K2015-99X-2273101-4), and FF was supported by the Medical Research Council (MC_PC_17164), the Oxford University Medical Research Fund (MRF/LSV2014/2091), King's College London (Challenge Award) and The Physiological Society (Formenti 2018). The authors disclosed that they do not have any conflicts of interest.s

MeSH headings: Pulmonary Circulation; Ventilation-Perfusion Ratio; Respiratory Distress Syndrome, Adult; Tomography, X-Ray Computed; Ventilator-Induced Lung Injury, Swine

Word count: 2,993

Abstract

Objective

Determine the intratidal regional gas and blood volume distributions at different levels of atelectasis in experimental collapse-prone lung injury. In this context, test the hypotheses that pulmonary aeration and blood volume matching is reduced during inspiration in the setting of fixed atelectasis, and that this mismatching is an important determinant of hypoxemia.

Design

Pre-clinical study.

Setting

Research laboratory.

Subjects

Seven anaesthetised pigs weight 28.7 (SD 2.1) kg.

Interventions

All animals received a saline-lavage surfactant depletion model of lung injury. Positive end-expiratory pressure (PEEP) was varied between 0 and 20 cmH_2O in a protocolized order to induce different levels of atelectasis.

Measurements and Main Results

Dynamic dual-energy computed tomography images of a juxtadiaphragmatic slice were obtained, gas and blood volume fractions within three gravitational regions calculated and normalized to lung tissue mass (V_N and Q_N respectively). Ventilatory conditions were

grouped based upon the fraction of lung mass that was atelectatic (FAM_{exp}<20%, 20-40% and ≥40%). Cyclical recruitment/derecruitment with FAM_{exp}≥40% was <7% of lung mass. In this group, inspiration-related increase in V_N was greater in the non-dependent (818 [95% confidence interval 729-908] μL/g) than in the dependent region (149[120-178] μL/g). Q_N decreased in inspiration in the non-dependent region (29[12-46] μL/g) and increased in the dependent region (39[30-48] μL/g). Inspiration-related changes in V_N and Q_N were negatively correlated in FAM_{exp}≥40% and 20-40% groups (r^2=0.56 and 0.40), but not in FAM_{exp}<20% group (r^2=0.01). Both the increase in Q_N in the dependent region and FAM_{exp} negatively correlated with PaO_2/FiO_2 ratio (ρ=-0.77 and -0.93 respectively).

Conclusions

In experimental fixed atelectasis, mechanical inspiratory breaths redistributed blood volume away from well-ventilated areas, worsening PaO_2/FiO_2.

Abstract word count: 266

Introduction

Mechanical ventilation is the mainstay of treatment in the acute respiratory distress syndrome (ARDS)(1) with refractory hypoxaemia remaining common(2). The optimal settings for mechanical ventilatory parameters, including positive end-expiratory pressure (PEEP), remain difficult to define on the individual patient basis(3). PEEP can significantly improve oxygenation in ARDS(4-6) and may mitigate ventilator-induced lung injury(7, 8) presumably through reducing cyclical alveolar recruitment/derecruitment (R/D). Conversely, PEEP reduces cardiac output(9, 10), can worsen overdistension injury of well-ventilated regions(3) and may increase mortality if titrated to open collapsed lung units(11). Most research aimed at setting the optimum mechanical ventilation parameters have focused on alveolar recruitment and lung compliance; fewer studies have investigated the role of these settings on regional distribution of pulmonary perfusion ($\dot{Q}$). Oxygenation is improved by pulmonary ventilation ($\dot{V}$) and $\dot{Q}$ matching, so $\dot{Q}$ should be considered throughout the respiratory cycle when titrating ventilation in ARDS.

Prolonged high inspiratory pressures may worsen oxygenation in patients(12) and in experimental lung injury(13) due to redistribution of blood towards dependent regions. Determining the regional distribution of blood during the time course of a single breath remains challenging. Dynamic dual-energy computed tomography (DECT)(14, 15) has the temporal resolution to address this.

DECT determines the fractions of three materials in a single voxel by imaging the same volume at two different X-ray photon energies(16). A series of simultaneous equations is then solved to quantify the *volume fraction* of each material within each voxel. In the context of pulmonary imaging, this three-material differentiation allows separation of gas, soft tissue and iodinated blood, which is not possible with classical single-energy scans. For example, if, after the administration of iodine contrast, a voxel on a single-energy scan has an attenuation of 0 Hounsfield Units (HU), it is impossible to determine whether it contains 100% water or a mixture of water, gas and iodine where the average density is 0 HU; DECT three-material differentiation solves this problem. Unfortunately, commercial DECT implementations are aimed towards qualitative interpretation of lung parenchymal blood content during apnoea, rather than the more physiological, continuous quantification within respiratory cycles.

We present here a novel three-material differentiation post-processing algorithm for DECT images that allows quantification of blood volume redistribution within single breaths. We validated this method *in vitro* and *in vivo*, and used it to study a collapse-prone lung injury pig model. We hypothesized that ventilatory conditions associated with significant atelectasis and minimal tidal recruitment (as would result from low PEEP in our model) would demonstrate worsening of gas (V) and blood volume (Q) matching during inspiration.

Materials and Methods

Animal experiments received ethics committee approval (Uppsala Regional Animal Research Ethics Committee ref. C98/16) and conformed with the ARRIVE(17) guidelines. For full experimental details see Supplementary Methods.

Experimental protocol

Seven domestic pigs (28.7 (2.1) kg; mean (SD)) were mechanically ventilated under general anaesthesia and a lung injury model induced by saline-lavage surfactant depletion. Animals were ventilated supine in a protocolized order covering PEEP steps from 5 to 20 cmH_2O, in 5 cmH_2O increments, and in reverse to 0 cmH_2O (from here on termed "ventilatory conditions"). Both limbs of the incremental/decremental PEEP protocol were studied in each animal. Respiratory rate was fixed at 10 breaths per minute, tidal volume 10 mL/kg and inspiratory:expiratory ratio 1:2. Single juxtadiaphragmatic slice DECT images of two complete respiratory cycles were obtained at 1 s intervals in each ventilatory condition. Images were segmented into three gravitational regions of equal height, and a post-processing algorithm applied to determine the mean volume fraction of gas, iodinated blood and soft tissue within each region.

Calculation of normalized gas and blood volumes

When the lung is inflated it expands in three dimensions, but only two of these dimensions are included within a single CT slice. Gas and blood volumes within each region were

therefore normalized to lung tissue mass: approximations for the whole lung gas and blood values were generated by multiplying by the ratio of the volume of the thoracic cavity to that of the slice. Whole lung equivalent values were then divided by the per-animal mean lung tissue mass within each region measured using volume CT scans.

Calculation of fractional atelectatic mass (FAM)

Whole lung volume DECT scans were obtained during end-expiratory breath holds in each ventilatory condition. Atelectatic subregions were defined as those regions with gas volume fraction ≤0.1 (equivalent to regions ≥-100 HU on single-energy non-contrast scans as previously described(18)). The masses of this subregion and the whole lung were calculated based upon their mean tissue densities (1–gas density) and respective volumes. The ratio of the two was termed whole lung fractional atelectatic mass in expiration (FAM_{exp}) and was used to divide the ventilatory conditions into three groups (FAM_{exp}<20%, 20-40% and ≥40%).

Statistical analyses

Comparisons between two groups were performed using *t*-test or Wilcoxon signed-rank test as appropriate, and those between three groups using Tukey's Honest Significant Differences test, with alpha adjustment for multiple comparisons. Correlation between independent and dependent variables was assessed with linear regression analysis following assessment of individual variables for normality and heteroscedasticity. Correlations involving FAM_{exp}

were examined using Spearman's rank correlation coefficient due to non-normality in FAM_{exp}.

Results

The DECT algorithm was validated *in vitro* and *in vivo* (Supplementary Materials). Briefly, the algorithm accurately predicted blood iodine concentrations *in vitro* (r^2=0.998; P<0.0001; n=4; Supplementary Fig.1) and provided reasonable agreement in lung volume changes *in vivo* compared with spirometry (r^2=0.92; mean error -33 [95% confidence interval -38 to -28] mL; n=8; Supplementary Fig.2), without being affected by cumulative iodine doses up to 9.2 g/kg or end-expiratory lung volumes between 166 and 1673 mL (Supplementary Fig.3). Single slice mean tissue density was correlated with, but consistently less than equivalent whole lung densities (r^2=0.97; relative decrease 14.3[13.4-15.2] %; n=7; Supplementary Fig.4); this difference was consistent between inspiration and expiration (n=5). The imaged slice moved caudally during inspiration by a mean of 3.21[2.76-3.66] mm and it never moved by a distance greater than the adjacent slice moving into the CT image (Supplementary Fig.5).

Baseline characteristics and cardiorespiratory variables

Mean pulmonary artery pressure always exceeded mean airway pressure (mean difference 20.3(7.2) mmHg). Mean cardiac output was 3.41(0.40) L/min, similar to the value of 3 L/min chosen to determine iodine contrast infusion rate. PEEP was positively correlated with peak airway pressure (P<0.0001; r^2=0.73) and negatively correlated with FAM_{exp} (P<0.0001;

r^2=0.74). Data points from each of the seven animals were included within each FAM_{exp} group. Supplementary Tables 1-3 present details of cardiorespiratory parameters grouped by animal, PEEP and FAM_{exp} respectively.

Effect of inspiration upon volume fractions of gas and iodinated blood

A gravitational effect on the distributions of gas, blood and soft tissue volumes within the slice was seen (Fig.1-2). Iodinated blood and soft tissue predominated in the dependent regions and gas in the non-dependent regions, this effect being more pronounced in the higher FAM_{exp} groups (Fig.2). During inspiration, gas volume fraction increased in all FAM_{exp} groups and all gravitational regions (all $P \leq 0.01$), and blood volume fraction decreased (all $P<0.005$). The effect of time into each individual scan sequence on iodinated blood volume fraction was minimal (increase of 0.0007 mL/cm^3/s; equivalent to 0.4 %/s; P=0.01; r^2=0.006).

Effect of FAM_{exp} upon normalized gas (V_N) and blood (Q_N) volumes in expiration

Expiratory V_N was greatest in the non-dependent region and least in the dependent region in all FAM_{exp} groups (Fig.3a; all adjusted $P<0.0006$), and significantly higher within all regions in the FAM_{exp}<20% group compared with the other two FAM_{exp} groups (all adjusted $P<0.0008$). Expiratory Q_N was greatest in the middle region in all FAM_{exp} groups (Fig.3b; all adjusted $P<0.0002$). Within-region, expiratory Q_N was always highest in the FAM_{exp}<20% group compared with the ≥40% group (all adjusted $P<0.027$). Similar effects were seen

when data were grouped via PEEP, with V_N and Q_N distributed within the low PEEP groups similarly to high FAM_{exp} groups and vice versa (Supplementary Fig.6).

Effects of inspiration upon normalized gas and blood volumes

Inspiration was associated with an increase in V_N within all regions in all FAM_{exp} groups (Fig.2; Fig.3c; all $P<0.0003$). The increase was greater in the non-dependent region compared with the dependent region in all cases ($P<0.0001$; Fig.3c). The $FAM_{exp}\geq40\%$ group demonstrated the greatest variation in regional ventilation between the non-dependent and dependent regions (818[729-908] µL/g versus 149[120-178] µL/g respectively; $P<0.0001$).

There was no inspiration-related change in Q_N in any region in the $FAM_{exp}<20\%$ group ($P=0.5$, 0.8 and 0.8; Fig.3d). In the FAM_{exp}20-40% group, inspiration increased Q_N in the dependent region by 26[13-38] µL/g ($P=0.01$). In the $FAM_{exp}\geq40\%$ group, Q_N decreased in the non-dependent (29[12-46] µL/g; $P=0.02$) and middle (28[13-44] µL/g; $P=0.01$) regions, but increased in the dependent region (39[30-48] µL/g; $P<0.001$). Total Q_N within the slice was not affected by inspiration (mean change in $FAM_{exp}<20\%$ group: 5[-1 to 12] µL/g; FAM_{exp} 20-40%: -1[-9 to 7] µL/g; $FAM_{exp}\geq40\%$: -6[-15 to 3] µL/g).

A negative relationship between regional ventilation and inspiratory Q_N increase was observed in the $FAM_{exp}\geq40\%$ (Fig.4; $r^2=0.56$) and FAM_{exp}20-40% ($r^2=0.40$) groups. FAM_{exp}

and the inspiratory Q_N increase in the dependent region were positively correlated (Spearman's ρ=0.79).

Effects upon PaO_2/FiO_2 (P/F) ratio

P/F ratio was negatively correlated with both FAM_{exp} (P<0.0001; ρ=-0.93) and inspiratory increase in Q_N in the dependent region (P<0.0001; ρ=-0.77). The relationships were non-linear in both cases (Fig.5). Following log-transformation of P/F ratio values, a linear relationship with FAM_{exp} was demonstrated (r^2=0.87).

Discussion

We found that inspiratory mechanical breaths at PEEP levels associated with clinically significant atelectasis and minimal tidal recruitment cause a redistribution of pulmonary parenchymal blood volume towards poorly ventilated regions in experimental collapse-prone lung injury. This phenomenon would increase shunt fraction beyond what would be expected from atelectasis alone, and may represent a significant causal component of the hypoxaemia observed with low-PEEP ventilation in ARDS(2).

Methodology developed for this study

We developed a novel DECT three-material differentiation algorithm to quantify gas and blood volume fractions at the voxel level. The iodine infusion protocol was designed to

ensure constant opacification of the entirety of the pulmonary vascular tree over the time course of the scan. There was very mild increase in measured iodine volume fractions throughout the scan period (0.4 %/s). The validity of the three-material differentiation algorithm was confirmed *in vivo* and *in vitro* (Supplementary Materials), and the normalization procedure to convert volume fractions of gas or blood to volumes per unit mass of lung tissue produced V_N values with a typical gravitational gradient (Fig.3a) and hysteresis (Supplementary Fig.6).

We demonstrate that, following normalization to regional lung tissue mass, the middle region of the lung had the highest blood volume (Fig.3b). This finding is in contrast to the classical result that perfusion and blood volume increase down the lung(19), where results are typically quoted in relationship to lung volume, rather than mass. Our results agree with recent results in human volunteers using MRI with arterial spin labelling, where perfusion per unit tissue mass was greatest in the middle gravitational region (6 mL/g/min) compared with the dependent and non-dependent regions (4-5 mL/g/min)(20). Overall, the validation performed with known iodine and gas volumes, and the similar gravitational distribution for normalized gas and blood volumes between our study and published data, demonstrate the usefulness of our technique and the dependability of the results.

Intra-tidal blood volume redistribution

In conditions with large volume atelectasis (≥40% of lung mass), we demonstrated minimal tidal recruitment (<7% of lung mass) based upon measures of atelectasis during breath holds

at end-inspiration and end-expiration. The majority of recruitment takes place over 4 s from the start of an end-inspiratory breath hold(21). Inspiratory time in our study was only 2 s, so it is likely that the FAM during end-inspiratory breath holds underestimates atelectasis during inspiration in tidal ventilation. It is possible that the already small cyclical R/D values reported here are still overestimates. Of note, the term 'fixed' represents atelectasis that demonstrates minimal change during one breath(22). The saline lavage model is classically described as recruitable in relation to the effects of PEEP rather than a single breath(23).

In conditions of large volume of relatively fixed atelectasis we demonstrated a reduction in Q_N within the non-dependent and middle regions associated with a reciprocal increase in the most-dependent region (Fig.3d), in the context of no inspiratory change in total Q_N. This suggests a cyclical redistribution of blood volume towards the most-dependent region during inspiration, then restored during expiration. These results are in contrast to those reported in an uninjured rabbit model, where blood volume redistributed from dependent to non-dependent regions in inspiration(24). Apart from anatomical differences between models, an explanation for these differences is that, unlike the earlier study, we studied a lung injury model and normalized the results to lung tissue mass.

The dependent region was ventilated least when significant atelectasis was present (Fig.3c), in keeping with results from electrical impedance tomography, where decreasing PEEP(25) or inspiratory time(26) shifts the centre of ventilation towards non-dependent regions. Inspiratory positive pressures may be delivered only to ventilated alveoli and the inspiration-associated decrease in alveolar vessel transmural pressure and volume only occurs in those

regions of the lung that are ventilated, and therefore redistribution of blood to non-ventilated regions is likely(13). As the oxygen reservoir within the lungs is highest during inspiration, this redistribution of blood volume would increase shunt fraction. This mechanism could explain why some patients exhibit hypoxaemia that is refractory to increases in inspired oxygen concentration and/or inspiratory time.

Effects of blood volume redistribution on oxygenation

Increase in CT-measured atelectasis has a negative relationship with oxygenation(27) and with the P/F log-transform(28), as confirmed here (Fig.5a). Moreover, we demonstrated a negative relationship between the increase in blood volume within the dependent region during inspiration and oxygenation (Fig.5b).

Due to multicollinearity between fixed atelectasis and intra-tidal pulmonary blood volume redistribution, identifying the relative contributions of these two determinants of hypoxaemia is challenging. This finding does raise an interesting question: is it the presence of atelectasis *per se* that leads to hypoxaemia in ARDS, or is intra-tidal redistribution of blood to atelectatic lung an additional requirement?

Limitations

We measured aeration and blood volume, surrogates of ventilation and perfusion. Regional ventilation can be derived using our technique, by measuring aeration in both inspiration and

expiration. Perfusion is more difficult to measure, however DECT-derived pulmonary blood volume can approximate perfusion (measured by contrast-bolus dynamic CT) with a mean correlation coefficient of 0.7(29).

We did not image the whole lung, but only one slice due to limitations in current technology. The slice we chose reasonably approximates the whole lung in terms of atelectatic fractions(30) and density distributions(31), and has been used to quantify atelectatic lung in both the uninjured animal(32, 33) and that with lung injury(22, 33). We demonstrated that whilst the single slice underestimated lung density, it did so by a consistent amount between inspiration and expiration such that our final outcome variables (change in V_N and Q_N) were likely similar to those seen for the whole lung (supplementary results). We demonstrated minimal caudal displacement of the imaged slice during inspiration at most equivalent to the next slice, whose make-up is unlikely to be substantially different, moving into the CT image.

The saline-lavage surfactant-depletion lung injury model demonstrates significant recoverability with both time since injury and application of high PEEP(23). As we used PEEP purely to generate differing amounts of atelectasis in the animals, any recovery was accounted for by the use of FAM_{exp} as a grouping variable, rather than PEEP itself. Additionally, we reversed the PEEP sequence in two animals to minimize any bias induced by recovery purely due to time from injury. The inherent effects of PEEP and inspiratory pressures upon regional blood volume may differ between models, however, and these results should be confirmed in other lung injury models.

Conclusions

We demonstrated a redistribution of pulmonary blood volume away from well-ventilated regions of lung during inspiration in experimental lung injury at PEEP levels associated with significant atelectasis and minimal cyclical R/D. This redistribution was associated with a clinically significant reduction in P/F ratio. This intra-tidal pulmonary blood volume redistribution has not previously been demonstrated during mechanical ventilation at clinically-relevant respiratory rates. It may be a putative explanation for the reduced PaO_2 seen in low PEEP ventilation in ARDS(2), and could potentially explain the large intra-tidal PaO_2 oscillations seen in experimental lung injury(22, 32, 34-36). Further work examining the optimum mechanical ventilatory strategies in ARDS should also examine the effects on pulmonary blood volume distribution, which is also relevant for oxygenation.

Acknowledgements

We are grateful to the staff at the Hedenstierna Laboratoriet and Radiology Department, Uppsala University Hospital including Agneta Roneus, Kerstin Ahlgren, Mariette Anderson, Liselotte Pihl, Maria Swälas and Monica Segelsjö for their expertise and technical assistance, Clive Hahn, Keith Dorrington, Peter Robbins and Jose Venegas for helpful discussions and Oxford Optronix Ltd for technical support. Finally, we are thankful to the unnamed reviewers who have provided highly constructive advice to improve this article.

Figure 1 Legend

Example source and post-processed images of a single juxtadiaphragmatic slice at PEEP 5 cmH_2O of pig's thorax during iodine infusion using the DECT algorithm. a) Composite source images representing a 30:70 merge of 80 kVp and 140 kVp images displayed using standard CT lung windows. b) Results of the DECT three-material differentiation algorithm for gas (blue), soft tissue (green) and iodinated blood (red) volume fractions. c) The DECT images following segmentation to include only lung parenchyma with the three gravitational regions of interest displayed. Typical expiration and inspiration images are shown in each case. A gravitational effect was seen within the slice with soft tissue and iodinated blood concentrated towards the dependent regions, with a reduction in volume fractions of these materials in inspiration.

Figure 2 Legend

Effects of inspiration on the volume fractions and normalized volumes of gas and iodinated blood within the juxtadiaphragmatic slice over the course of two respiratory cycles. Results are presented for the three different gravitational regions of the studied slice and grouped by fractional atelectatic mass of the lung in expiration (FAM_{exp}). Airway pressure traces are provided for comparison, and grey background denotes inspiration. In all regions and all FAM_{exp} groups gas volume fraction and normalized gas volume increased ($P \leq 0.01$) and blood volume fraction decreased ($P < 0.005$) during inspiration. The effects of inspiration on normalized blood volume were most pronounced in the $FAM_{exp} \geq 40\%$ group, with normalized blood volume decreasing in the middle and non-dependent regions and increasing in the dependent region. Points represent mean and SEM for clarity of the figure.

Figure 3 Legend

Expiratory normalized gas (V_N; a) and blood volumes (Q_N; b) within each region, and fractional expiratory mass of the lung in expiration (FAM_{exp}) grouping. c) Effects of an inspiratory breath upon V_N. In the higher FAM_{exp} groups there is relatively less ventilation occurring in the dependent regions. d) Effects of an inspiratory breath upon Q_N. Minimal change was seen in normalized blood volume in the $FAM_{exp} < 20\%$ group, however in the other conditions the normalized blood volume in the dependent region increased and those in the others decreased with inspiration. Points represent mean and either SD (a,b) or 95% confidence interval of change (c,d).

Figure 4 Legend

Relationship between the inspiratory change in normalized gas (V_N) and blood (Q_N) volumes dependent upon fraction of the mass of the entire lung that was atelectatic in expiration (FAM_{exp}). For $FAM_{exp} < 20\%$ minimal relationship was seen, however within the other two groups there was a clear negative relationship: those regions with the least ventilation received an increase in blood volume and those with the most ventilation a decrease, suggestive of an inspiration-related redistribution that worsened ventilation-perfusion matching.

Figure 5 Legend

Effect of atelectasis (a) and intra-tidal normalized blood volume redistribution towards the dependent region (b) upon PaO_2/FiO_2 (P/F) ratio. P/F ratio was negatively correlated with both measures in a non-linear fashion (Spearman's ρ=-0.93 and -0.77 respectively) and the log-transform of P/F ratio was linearly related to atelectasis (r^2=0.87). Box-and-whiskers plots represent median, inter-quartile range and range for the three different FAM_{exp} groups studied (a) and between those conditions that demonstrated either an inspiration-related reduction or increase in blood volume in the dependent region (b).

Supplementary File 1 Legend

Extra methodology including in-depth description of the DECT three-material decomposition algorithm, normalization procedure and validation experiments. Results of the validation experiments and analysis of slice movement during ventilation.

References

1. Slutsky AS, Ranieri VM. Ventilator-induced lung injury. N Engl J Med 2013;369(22):2126-2136.

2. Goligher EC, Kavanagh BP, Rubenfeld GD, et al. Oxygenation response to positive end-expiratory pressure predicts mortality in Acute Respiratory Distress Syndrome. A secondary analysis of the LOVS and ExPress trials. Am J Respir Crit Care Med 2014;190(1):70-76.

3. Sahetya SK, Goligher EC, Brower RG. Fifty years of research in ARDS. Setting positive end-expiratory pressure in Acute Respiratory Distress Syndrome. Am J Respir Crit Care Med 2017;195(11):1429-1438.

4. Ashbaugh DG, Bigelow DB, Petty TL, et al. Acute respiratory distress in adults. Lancet 1967;2(7511):319-323.

5. Mercat A, Richard JM, Vielle B, et al. Positive end-expiratory pressure setting in adults with acute lung injury and acute respiratory distress syndrome: A randomized controlled trial. JAMA 2008;299(6):646-655.

6. Meade MO, Cook DJ, Guyatt GH, et al. Ventilation strategy using low tidal volumes, recruitment maneuvers, and high positive end-expiratory pressure for acute lung injury and acute respiratory distress syndrome: a randomized controlled trial. JAMA 2008;299(6):637-645.

7. Villar J, Kacmarek RM, Perez-Mendez L, et al. A high positive end-expiratory pressure, low tidal volume ventilatory strategy improves outcome in persistent acute

respiratory distress syndrome: a randomized, controlled trial. Crit Care Med 2006;34(5):1311-1318.

8. Amato MBP, Barbas CS, Medeiros DM, et al. Effect of a protective-ventilation strategy on mortality in the acute respiratory distress syndrome. N Engl J Med 1998;338.

9. Fougeres E, Teboul JL, Richard C, et al. Hemodynamic impact of a positive end-expiratory pressure setting in acute respiratory distress syndrome: importance of the volume status. Crit Care Med 2010;38(3):802-807.

10. Dantzker DR, Lynch JP, Weg JG. Depression of cardiac output is a mechanism of shunt reduction in the therapy of acute respiratory failure. Chest 1980;77(5):636-642.

11. Cavalcanti AB, Suzumura EA, Laranjeira LN, et al. Effect of lung recruitment and titrated positive end-expiratory pressure (PEEP) vs low PEEP on mortality in patients with Acute Respiratory Distress Syndrome: a randomized clinical trial. JAMA 2017;318(14):1335-1345.

12. Villagra A, Ochagavia A, Vatua S, et al. Recruitment maneuvers during lung protective ventilation in Acute Respiratory Distress Syndrome. Am J Respir Crit Care Med 2002;165(2):165-170.

13. Musch G, Harris RS, Vidal Melo MF, et al. Mechanism by which a sustained inflation can worsen oxygenation in acute lung injury. Anesthesiology 2004;100(2):323-330.

14. Thieme SF, Hoegl S, Nikolaou K, et al. Pulmonary ventilation and perfusion imaging with dual-energy CT. Eur Radiol 2010;20(12):2882-2889.

15. Thieme SF, Johnson TRC, Lee C, et al. Dual-Energy CT for the Assessment of Contrast Material Distribution in the Pulmonary Parenchyma. AJR Am J Roentgenol 2009;193(1):144-149.

16. McCollough CH, Leng S, Yu L, et al. Dual- and multi-energy CT: principles, technical approaches, and clinical applications. Radiology 2015;276(3):637-653.

17. Kilkenny C, Browne WJ, Cuthill IC, et al. Improving bioscience research reporting: the ARRIVE guidelines for reporting animal research. PLOS Biology 2010;8(6):e1000412.

18. Gattinoni L, Pesenti A, Bombino M, et al. Relationships Between Lung Computed Tomographic Density, Gas Exchange, and PEEP in Acute Respiratory Failure. Anesthesiology 1988;69(6):824-832.

19. Hedenstierna G, White FC, Mazzone R, et al. Redistribution of pulmonary blood flow in the dog with PEEP ventilation. J Appl Physiol 1979;46(2):278-287.

20. Hopkins SR, Henderson AC, Levin DL, et al. Vertical gradients in regional lung density and perfusion in the supine human lung: the Slinky effect. J Appl Physiol 2007;103(1):240-248.

21. Neumann P, Berglund JE, Mondéjar EF, et al. Dynamics of lung collapse and recruitment during prolonged breathing in porcine lung injury. J Appl Physiol 1998;85(4):1533-1543.

22. Crockett DC, Cronin JN, Bommakanti N, et al. Tidal changes in PaO2 and their relationship to cyclical lung recruitment/derecruitment in a porcine lung injury model. Br J Anaesth 2019;122(2):277-285.

23. Ballard-Croft C, Wang D, Sumpter LR, et al. Large-Animal Models of Acute Respiratory Distress Syndrome. Ann Thorac Surg 2012;93(4):1331-1339.

24. Porra L, Broche L, Degrugilliers L, et al. Synchrotron imaging shows effect of ventilator settings on intrabreath cyclic changes in pulmonary blood volume. Am J Respir Cell Mol Biol 2017;57(4):459-467.

25. Zick G, Elke G, Becher T, et al. Effect of PEEP and tidal volume on ventilation distribution and end-expiratory lung volume: a prospective experimental animal and pilot clinical study. PloS one 2013;8(8):e72675.

26. Boehme S, Bentley AH, Hartmann EK, et al. Influence of Inspiration to Expiration Ratio on Cyclic Recruitment and Derecruitment of Atelectasis in a Saline Lavage Model of Acute Respiratory Distress Syndrome. Crit Care Med 2015;43(3):e65-e74.

27. Markstaller K, Kauczor HU, Weiler N, et al. Lung density distribution in dynamic CT correlates with oxygenation in ventilated pigs with lavage ARDS. Br J Anaesth 2003;91(5):699-708.

28. Reske AW, Costa ELV, Reske AP, et al. Bedside estimation of nonaerated lung tissue using blood gas analysis. Crit Care Med 2013;41(3):732-743.

29. Kay FU, Beraldo MA, Nakamura MAM, et al. Quantitative dual-energy computed tomography predicts regional perfusion heterogeneity in a model of acute lung injury. J Comput Assist Tomogr 2018;42(6):866-872.

30. Bletz C, Markstaller K, Karmrodt J, et al. Quantification of atelectases in artificial respiration: spiral-CT versus dynamic single-slice CT. RoFo : Fortschritte auf dem Gebiete der Rontgenstrahlen und der Nuklearmedizin 2004;176(3):409-416.

31. Zinserling J, Wrigge H, Neumann P, et al. Methodologic aspects of attenuation distributions from static and dynamic thoracic CT techniques in experimental acute lung injury. Chest 2005;128(4):2963-2970.

32. Formenti F, Bommakanti N, Chen R, et al. Respiratory oscillations in alveolar oxygen tension measured in arterial blood. Sci Rep 2017;7(1):7499.

33. David M, Karmrodt J, Bletz C, et al. Analysis of atelectasis, ventilated, and hyperinflated lung during mechanical ventilation by dynamic CT. Chest 2005;128(5):3757-3770.

34. Baumgardner JE, Markstaller K, Pfeiffer B, et al. Effects of respiratory rate, plateau pressure, and positive end-expiratory pressure on PaO2 oscillations after saline lavage. Am J Respir Crit Care Med 2002;166(12 Pt 1):1556-1562.

35. Formenti F, Chen R, McPeak H, et al. Intra-breath arterial oxygen oscillations detected by a fast oxygen sensor in an animal model of acute respiratory distress syndrome. Br J Anaesth 2015;114(4):683-688.

36. Williams EM, Viale JP, Hamilton RM, et al. Within-breath arterial PO2 oscillations in an experimental model of acute respiratory distress syndrome. Br J Anaesth 2000;85(3):456-470.

Figure 1

Click here to access/download;Figure;fig1.tiff

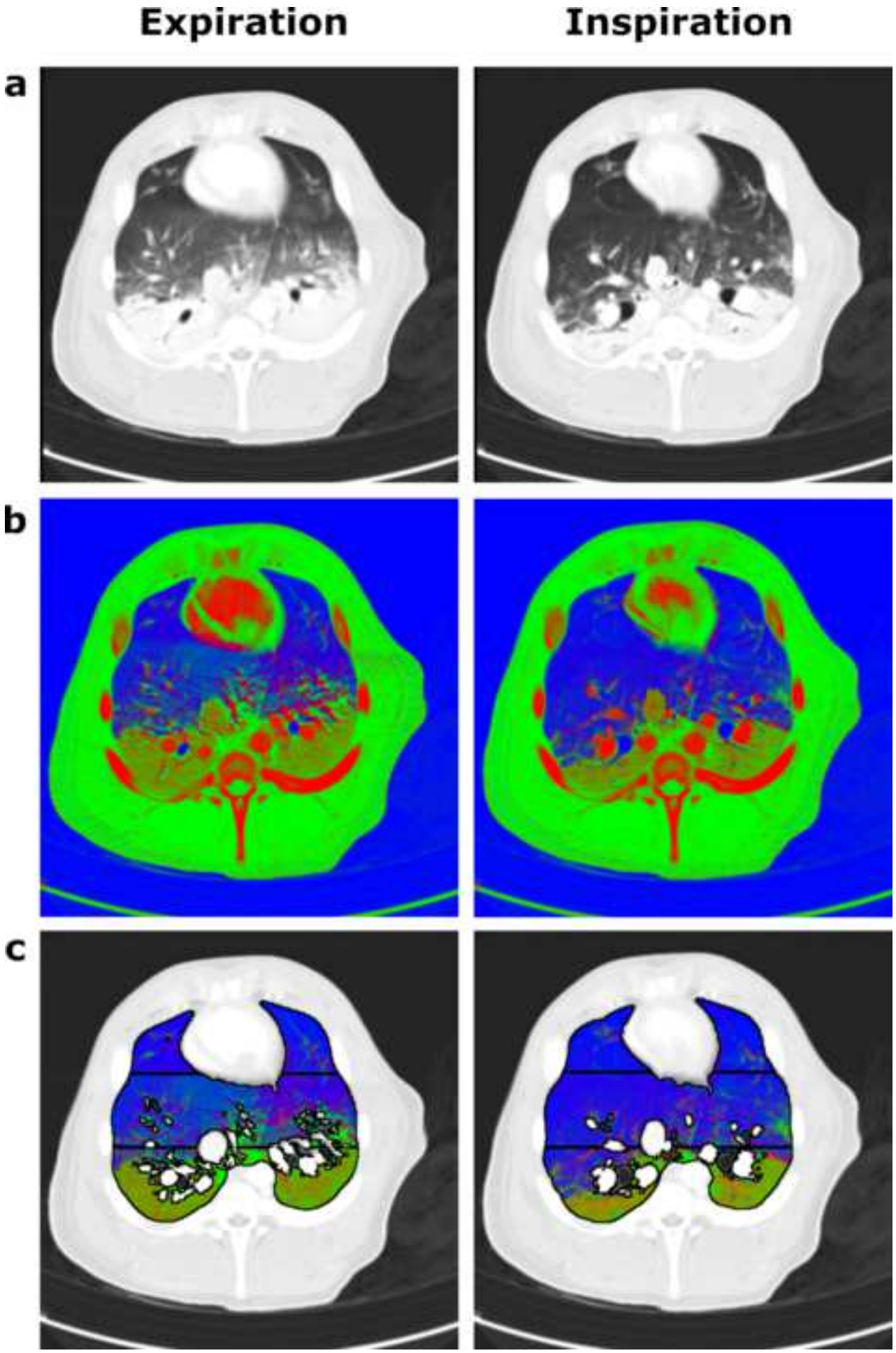

Figure 2

Click here to access/download;Figure;fig2.tiff

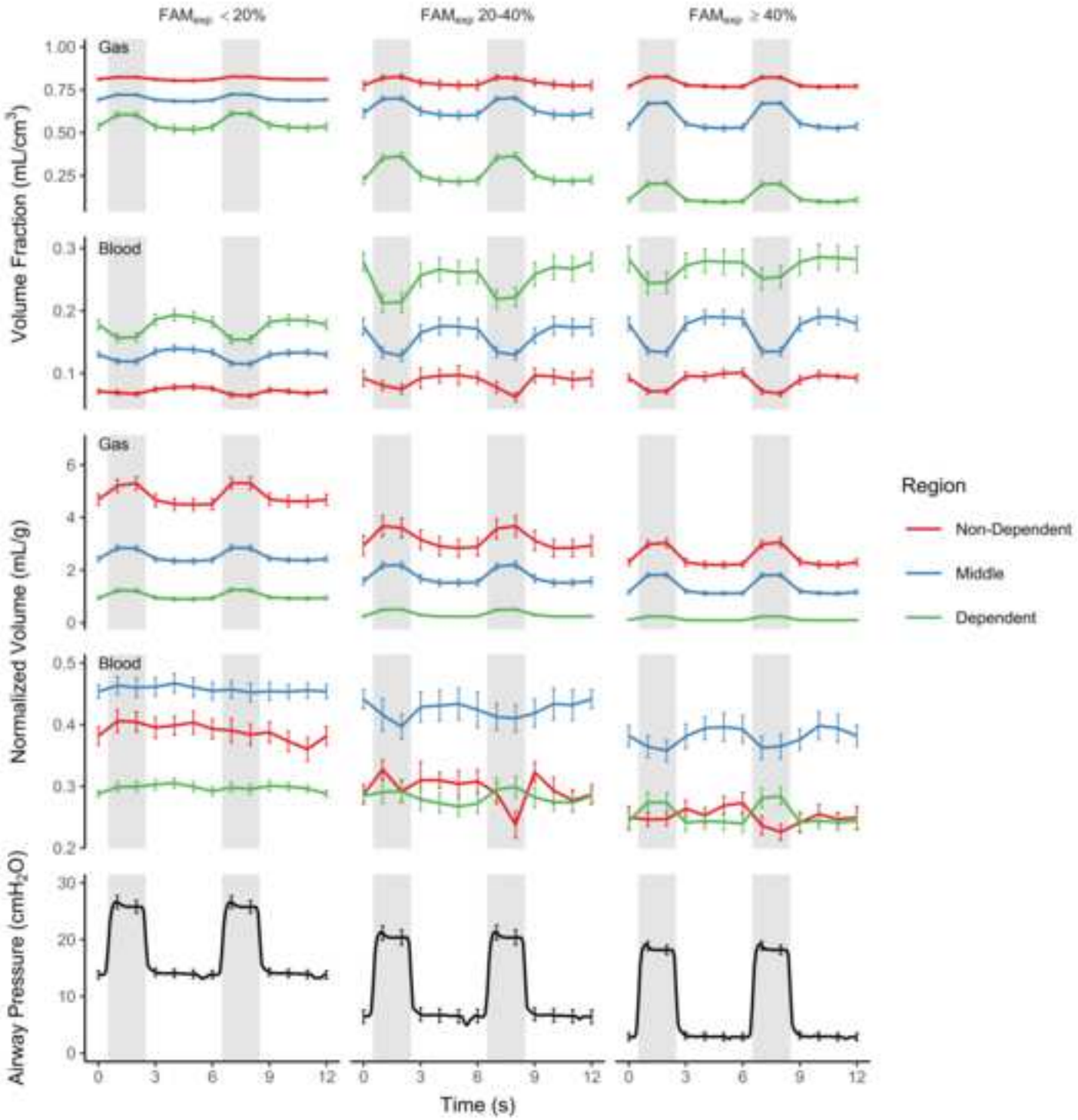

Figure 3

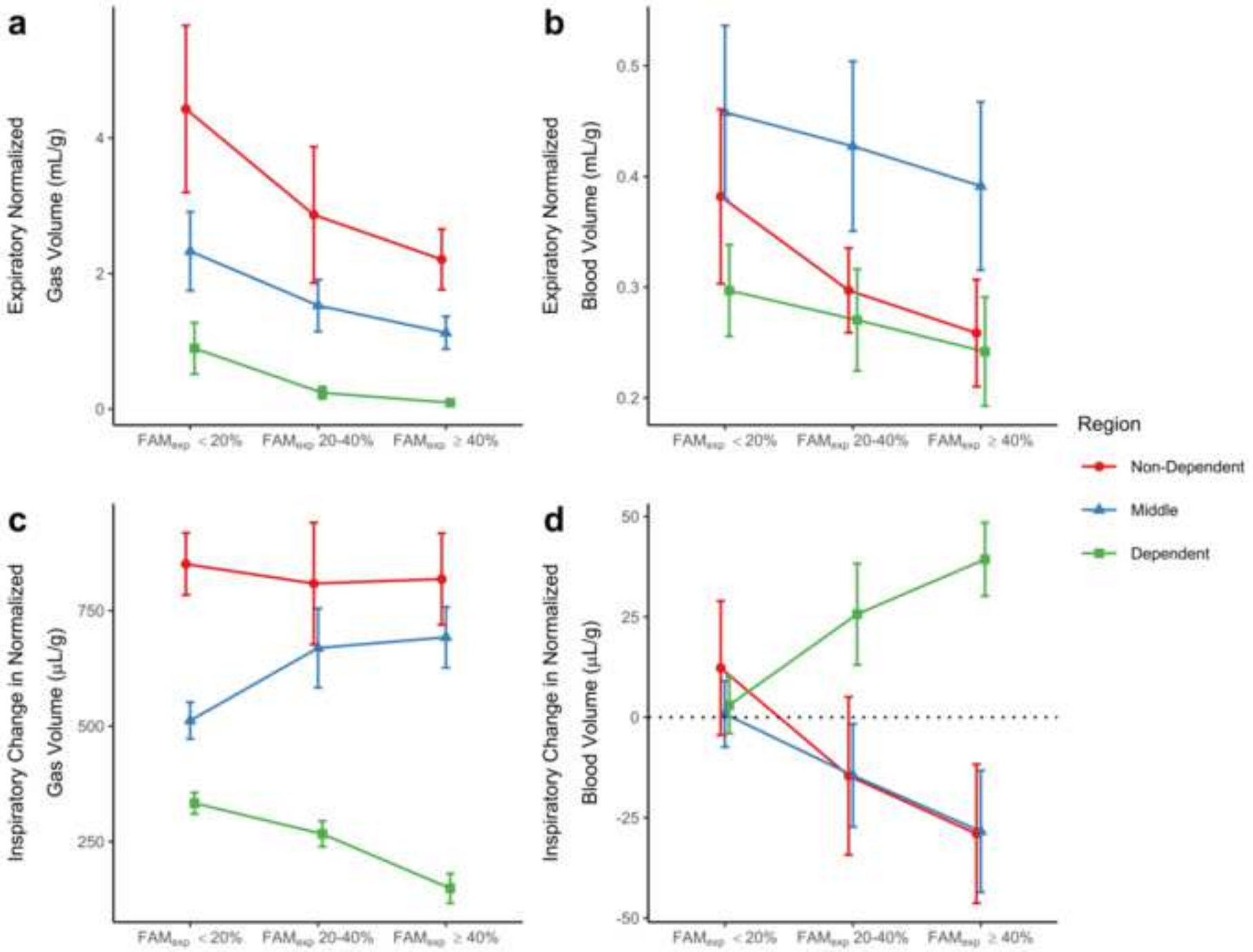

Figure 4

Click here to access/download;Figure;fig4.tiff

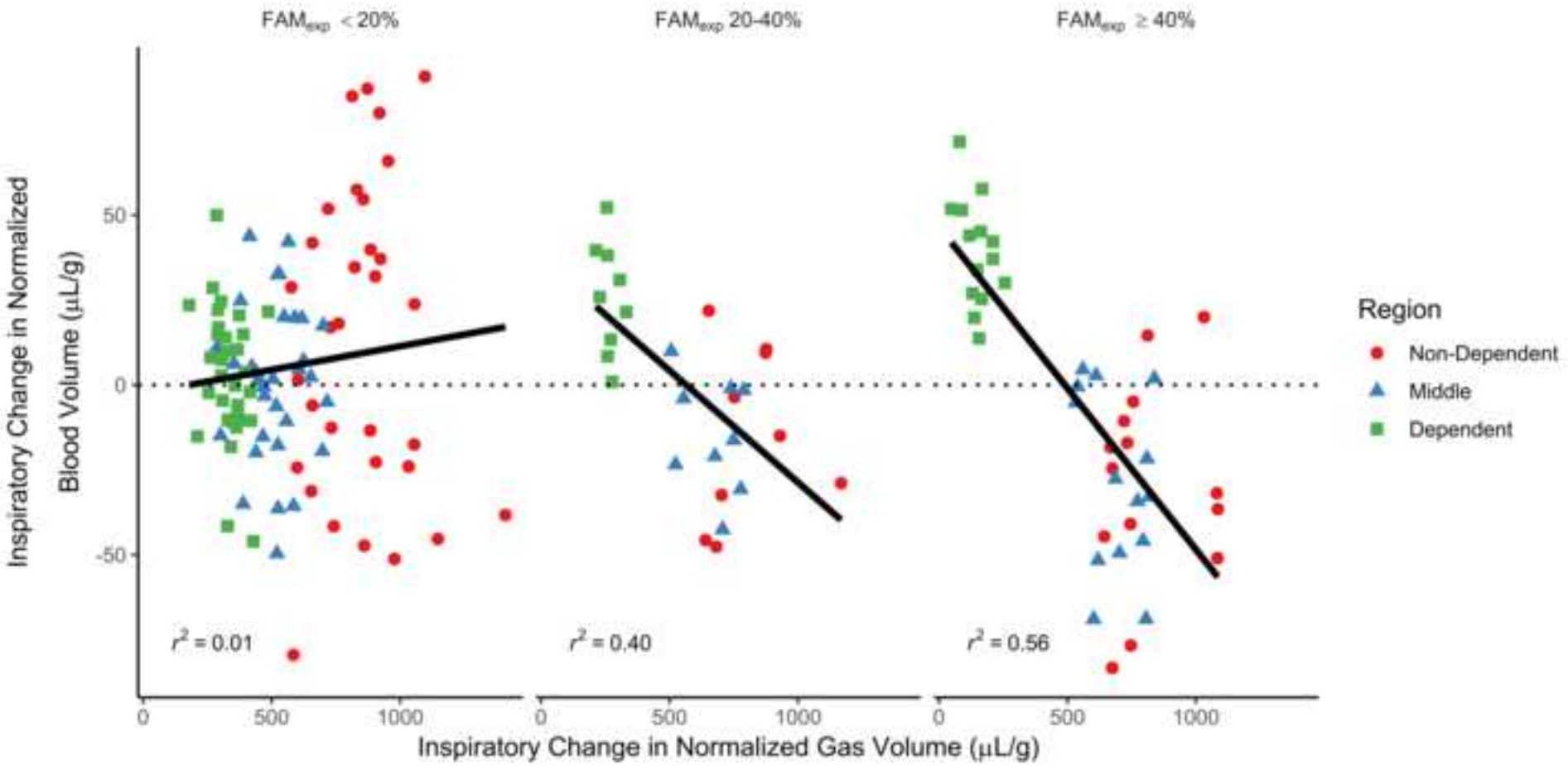

Figure 5

Click here to access/download;Figure;fig5.tiff

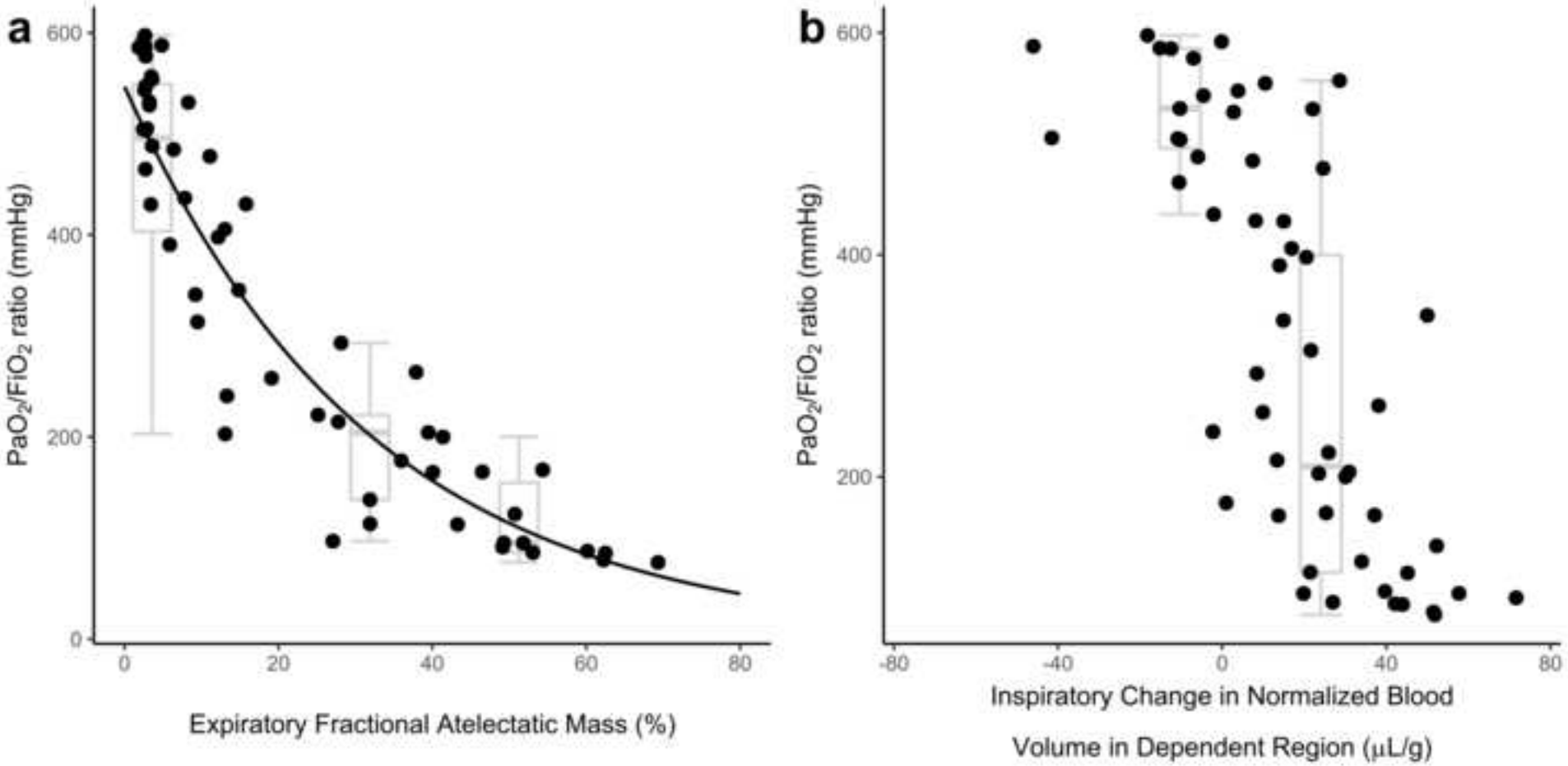

Supplemental Materials